

## Crystal and Molecular Structures of Disilyl Sulphide (at 120 K) and of Disilyl Selenide (at 125 K) and Comparison with Crystalline Disilyl Oxide

By Michael J. Barrow\* and E. A. V. Ebsworth, Department of Chemistry, Edinburgh University, West Mains Road, Edinburgh EH9 3JJ

Crystals of  $\text{SiH}_3\text{-S-SiH}_3$  (at 120 K) are orthorhombic, space group  $Pbcn$ , with  $a = 8.14$ ,  $b = 14.76$ ,  $c = 8.68$  Å [estimated standard deviations (e.s.d.s) 0.3% assumed] and  $Z = 8$ . Crystals of  $\text{SiH}_3\text{-Se-SiH}_3$  (at 125 K) are tetragonal, space group  $P4_32_12$ , with  $a = 8.36$  Å (e.s.d. 0.4% assumed),  $c = 15.4$  Å (e.s.d. 0.6% assumed), and  $Z = 8$ . Crystals were grown 'in situ' on a Weissenberg goniometer fitted with low-temperature equipment. Using photographic (microdensitometer) intensities the structures have been refined to  $R = 0.038$  over 410 reflexions ( $\text{SiH}_3\text{-S-SiH}_3$ ), and  $R = 0.055$  over 263 reflexions ( $\text{SiH}_3\text{-Se-SiH}_3$ ). The heavy-atom geometries are  $\langle\text{Si-S}\rangle = 2.142(7)$  Å with  $\text{Si-S-Si} = 98.4(3)^\circ$ , and  $\langle\text{Si-Se}\rangle = 2.27(2)$  Å with  $\text{Si-Se-Si} = 95.7(5)^\circ$ . There is specific molecular alignment in both crystal structures giving rise to  $\text{Si}\cdots\text{S}$  (or  $\text{Se}$ ) intermolecular interactions; the lengths of these contacts are 0.35–0.4 Å less than the sum of van der Waals radii. In both structures each Si atom has 4 + 1 co-ordination while the S (or Se) atoms have 2 + 2 co-ordination; this is in contrast to crystalline  $\text{SiH}_3\text{-O-SiH}_3$  where only one Si atom is involved in an intermolecular contact to oxygen.

A POTENTIAL-ENERGY (p.e.) function for the Si-O-Si angle bend in  $\text{SiH}_3\text{-O-SiH}_3$  has been deduced from an analysis of the Raman spectrum.<sup>1</sup> This function has a minimum at  $\text{Si-O-Si} = 149^\circ$  but the hump at the linear configuration corresponds to only 112  $\text{cm}^{-1}$ . The possibility arises here that the angle in the solid could be very different from the angle of  $144.1(9)^\circ$  determined by gas-phase electron diffraction (e.d.);<sup>2</sup> crystal packing forces could easily deform the heavy-atom geometry. Yet, a recent X-ray crystal structure<sup>3</sup> reports an angle of  $142.2(3)^\circ$ , surprisingly close to the e.d. value and to the minimum of the p.e. function. Rather, the X-ray analysis points to another aspect of the structural chemistry of  $\text{SiH}_3\text{-O-SiH}_3$  since the molecules are aligned in the crystal to form directionally specific intermolecular  $\text{O}\cdots\text{Si}$  contacts of length 3.12(1) Å, 0.5 Å less than the sum of van der Waals radii. These interactions, although strong enough to cause molecular alignment, seem too weak to affect the *intra*-molecular geometry but nevertheless suggest incipient five-co-ordination at silicon.

The next two members of the disilyl chalcogenides,  $\text{SiH}_3\text{-S-SiH}_3$  and  $\text{SiH}_3\text{-Se-SiH}_3$ , have no unusual spectroscopic properties. The angles at S and Se, determined by electron diffraction in the gas phase, are  $97.4(7)$  and  $96.6(7)^\circ$  respectively.<sup>4,5</sup> There have been no previous reports of intermolecular  $\text{S}\cdots\text{Si}$  or  $\text{Se}\cdots\text{Si}$  interactions in the crystalline state, yet the possibilities for such features in the crystalline sulphide and selenide species demand investigation, if only because the narrowness of the angles at S and Se make these atoms even more accessible than oxygen in disilyl oxide. We now report the results of X-ray investigations for crystals of disilyl sulphide and disilyl selenide.

### EXPERIMENTAL

*Crystal data.*—(a) *Disilyl sulphide.*  $\text{SiH}_3\text{-S-SiH}_3$ ,  $M = 94.3$ , m.p. 195 K. At 120 K crystals are orthorhombic,  $a = 8.14$ ,  $b = 14.76$ ,  $c = 8.68$  Å [estimated standard deviations (e.s.d.s) 0.3% assumed],  $U = 1\ 042.9$  Å<sup>3</sup>,  $Z = 8$ ,  $D_c = 1.20$  g  $\text{cm}^{-3}$ ,  $\text{Cu-K}\alpha$  radiation (nickel filter),

$\lambda = 1.5418$  Å,  $\mu(\text{Cu-K}\alpha) = 84.6$   $\text{cm}^{-1}$ , space group  $Pbcn$  ( $D_{2h}^{14}$ , no. 60) by systematic absences.

The final least-squares weighting scheme was  $w^{-1} = 1 + 0.002(F_o - 30)^2$  and the final value of an isotropic extinction coefficient was  $g = 28(5) \times 10^{-7}$ , where  $F_o' = F_o[1 - (gF_o^2/\sin\theta)]$ . A final difference-Fourier synthesis showed no peaks or troughs outside the range  $\pm 0.3$  e Å<sup>-3</sup>. Final values of the discrepancy indices, over 410 reflexions, were  $R = \Sigma|\Delta|/\Sigma|F_o| = 0.038$  and  $R' = (\Sigma w\Delta^2/\Sigma wF_o^2)^{1/2} = 0.047$ .

(b) *Disilyl selenide.*  $\text{SiH}_3\text{-Se-SiH}_3$ ,  $M = 141.2$ , m.p. 195 K. At 125 K crystals are tetragonal,  $a = 8.36$ ,  $c = 15.4$  Å (e.s.d.s 0.4% assumed for  $a$ , 0.6% assumed for  $c$ ),  $U = 1\ 076.3$  Å<sup>3</sup>,  $Z = 8$ ,  $D_c = 1.74$  g  $\text{cm}^{-3}$ ,  $\text{Cu-K}\alpha$  radiation (nickel filter),  $\lambda = 1.5418$  Å,  $\mu(\text{Cu-K}\alpha) = 126.1$   $\text{cm}^{-1}$ , space group  $P4_32_12$  ( $D_4^8$ , no. 96) by systematic absences and analysis.

The final least-squares weighting scheme was  $w^{-1} = 1 + 0.0003(40 - F_o)^2$  for  $F_o < 40$ , and  $w^{-1} = 1 + 0.0002(F_o - 40)^2$  for  $F_o \geq 40$ . The final value of the isotropic extinction coefficient was  $g = 49(10) \times 10^{-7}$ . A final difference-Fourier synthesis showed no peaks or troughs outside the range  $\pm 0.6$  e Å<sup>-3</sup>. Final values of the discrepancy indices, over 263 reflexions, were  $R = 0.055$  and  $R' = 0.067$ .

*Procedure.*—Both compounds are air- and moisture-sensitive liquids at room temperature. Pure samples were sealed in thin-walled Pyrex glass capillaries and mounted on goniometer heads using heat-insulating Tufnol insets. Single crystals were grown 'in situ' on a Nonius Weissenberg goniometer. The goniometer was fitted with Nonius low-temperature nitrogen-gas-stream equipment with some locally devised modifications. Intensity films were exposed using copper X-radiation and the multiple-film-pack equi-inclination Weissenberg method.

Two different crystals of  $\text{SiH}_3\text{-S-SiH}_3$  were used for intensity data: crystal (1) for the Weissenberg levels  $hk0$ —4, and crystal (2) for the levels  $hk0$ —1 and  $hk5$ —6. (The duplicated  $hk0$  and  $hk1$  data were merged together after data reduction.) Both crystals were grown inside the same capillary which had an external diameter of 0.39 mm. During intensity photography a thin sheet of nickel foil was used as a diffracted beam filter (in addition to the incident beam nickel filter) to reduce the background from X-ray fluorescence.

It proved difficult to grow suitable crystals of  $\text{SiH}_3\text{-Se-}$

$\text{SiH}_3$ . The crystal eventually used for data collection was grown inside a fairly wide capillary (external diameter 0.62 mm). This crystal was aligned with  $c$  along the camera axis. There were small randomly orientated crystallites associated with the main crystal, and additional problems arose from the pronounced X-ray absorption and fluorescence. Even though the fluorescence was minimised by using a thin sheet of zinc foil as a diffracted beam filter (in addition to the incident beam nickel filter) the background radiation level was still high. Intensity films were exposed for the Weissenberg levels  $hk0-8$ , with exposure times increasing to 4 days for  $hk8$ . At this stage data collection was stopped. Attempts were made to grow another crystal, this time aligned along  $a$ , but without success.

Integrated film intensities were derived from microdensitometer measurements performed by the S.R.C. Microdensitometer Service at Daresbury Laboratory, Warrington. The data were corrected for absorption effects using the SHELX program:<sup>6</sup> for each crystal a sufficient number of faces were defined to approximate the required (cylindrical) shape and orientation. The intensities were further corrected for Lorentz and polarisation effects. After merging equivalent reflexions there remained 412 unique observed intensities for  $\text{SiH}_3\text{-S-SiH}_3$  ( $hkl$  only: centrosymmetric space group), and 266 unique observed intensities ( $hkl$  and  $\bar{h}\bar{k}\bar{l}$ : non-centrosymmetric space group) for  $\text{SiH}_3\text{-Se-SiH}_3$ . During subsequent calculations rather poor agreement between  $F_o$  and  $F_c$  was noticed in the case of two reflexions (915 and 796) in the sulphide data and for three reflexions (220, 225, and 476) in the selenide data. These reflexions were removed from the data sets so that the structure analyses are based on 410 reflexions ( $\text{SiH}_3\text{-S-SiH}_3$ ) and 263 reflexions ( $\text{SiH}_3\text{-Se-SiH}_3$ ).

**Structure Solution.**—For neither of the structures do the space groups impose any restriction on the molecular symmetry for  $Z = 8$ .

The S and Si atoms in the sulphide structure were located from a sharpened Patterson synthesis.

The space group  $P4_12_12$  (or its enantiomer  $P4_32_12$ ) was not unambiguously indicated by the systematic absences for crystalline  $\text{SiH}_3\text{-S-SiH}_3$  since the  $00l$  reflexions had not been recorded. Other possible space groups were  $P4_22_12$  and  $P4_2m$  although both seemed unlikely from packing considerations. A sharpened Patterson function strongly suggested space group  $P4_12_12$  and indicated coordinates for the Se atom. The Si atoms were located from an  $F_o$  Fourier synthesis.

**Refinement.**—Both structures were refined by least-squares calculations to minimise the quantity  $\sum w(|F_o| - |F_c|)^2$ . Inter-layer scale factors were varied during the initial isotropic refinement but thereafter held constant with only a single overall scale factor varied during the anisotropic refinement. Hydrogen atoms were located from difference-Fourier syntheses. For the sulphide structure, hydrogen parameters (including individual isotropic temperature factors) were included in the refinement process although H(13) adopted a high temperature factor,  $U = 0.17 \text{ \AA}^2$ , which would never fully converge. The hydrogen peaks in the difference-Fourier synthesis of  $\text{SiH}_3\text{-S-SiH}_3$  were rather diffuse. These hydrogens were included in the model at positions determined from the difference map but their parameters were not refined.

Least-squares weighting schemes and isotropic extinction corrections were included during the later stages of refinement (see crystal data above). Towards the end of cal-

culations on  $\text{SiH}_3\text{-S-SiH}_3$ , comparative least-squares refinements were performed to distinguish between the alternative space group enantiomer structures. Values of the discrepancy indices,  $P4_12_12$  vs.  $P4_32_12$ , were:  $R = 0.0556$  vs.  $0.0550$ ,  $R' = 0.0674$  vs.  $0.0669$ . The test favours  $P4_12_12$  and that is the structure presented here.

Atomic scattering factors for Se were taken from ref. 7, for Si and S from ref. 8, and for H from ref. 9. The  $\Delta f'$  and  $\Delta f''$  corrections for Se, Si, and S atoms were from ref. 10. Calculations were performed using computers of the Edinburgh Regional Computing Centre and using programs written here together with the program systems X-RAY 76,<sup>11</sup> SHELX,<sup>6</sup> and PLUTO.<sup>12</sup>

## RESULTS

Final values of atomic parameters for disilyl sulphide and disilyl selenide are given in Tables 1 and 2 respectively. Details of the intramolecular geometries are given in Table 3 and the intermolecular geometries in Table 4. Tables of observed and calculated structure factors and of atomic thermal parameters are available as Supplementary Publication No. SUP 23153 (8 pp.).\* Figures 1–3 show the structure of  $\text{SiH}_3\text{-S-SiH}_3$ , Figures 4–7 the structure of  $\text{SiH}_3\text{-Se-SiH}_3$ , and Figures 8 and 9 that of  $\text{SiH}_3\text{-O-SiH}_3$  (for comparison).

The cell parameters are subject to the usual errors associated with the Weissenberg film method. These errors are probably accentuated by the use of split-film cassettes for low-temperature work, and in the case of the selenide crystal by the other problems mentioned before. Estimated standard deviations given in Tables 1–4 do

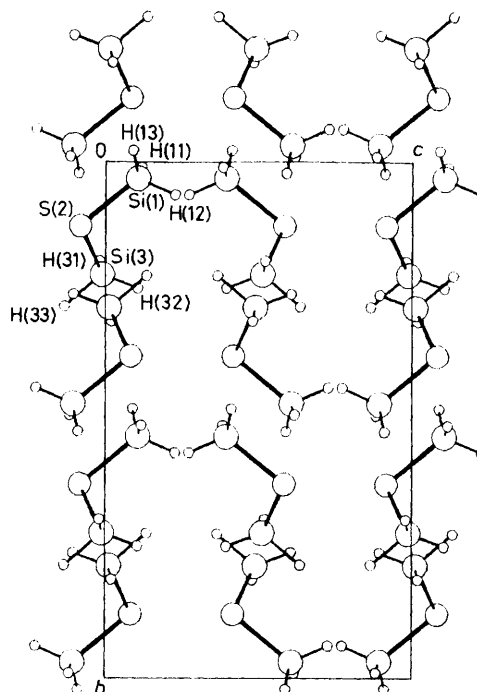


FIGURE 1 Arrangement of molecules in the unit cell of  $\text{SiH}_3\text{-S-SiH}_3$  viewed down  $a$

\* For details see Notices to Authors No. 7, *J. Chem. Soc., Dalton Trans.*, 1981, Index issue.

TABLE 1

Atomic parameters for SiH<sub>3</sub>-S-SiH<sub>3</sub> (with estimated standard deviations in parentheses)

Atom	<i>x/a</i>	<i>y/b</i>	<i>z/c</i>
Si(1)	0.257 60(23)	0.031 32(11)	0.105 76(26)
S(2)	0.275 08(21)	0.124 25(10)	-0.083 06(23)
Si(3)	0.089 55(21)	0.218 10(12)	-0.011 63(29)
H(11)	0.103(8)	0.010(5)	0.117(10)
H(12)	0.309(10)	0.062(5)	0.227(12)
H(13)	0.392(17)	-0.022(9)	0.089(19)
H(31)	-0.061(9)	0.192(5)	-0.020(10)
H(32)	0.127(13)	0.244(6)	0.105(14)
H(33)	0.107(11)	0.280(6)	-0.134(11)

TABLE 2

Atomic parameters for SiH<sub>3</sub>-Se-SiH<sub>3</sub> (with estimated standard deviations in parentheses)

Atom	<i>x/a</i>	<i>y/b</i>	<i>z/c</i>
Si(1)	0.227 5(9)	0.339 9(9)	0.338 6(9)
Se(2)	0.209 8(3)	0.135 7(3)	0.243 5(3)
Si(3)	0.396 7(9)	0.233 7(9)	0.148 7(8)
H(11)*	0.38	0.38	0.36
H(12)*	0.12	0.46	0.30
H(13)*	0.17	0.24	0.39
H(31)*	0.51	0.22	0.20
H(32)*	0.35	0.38	0.12
H(33)*	0.35	0.19	0.06

\* Hydrogen atoms located from difference map and not refined.

TABLE 3

Intramolecular geometries for SiH<sub>3</sub>-Y-SiH<sub>3</sub>

(a) Interatomic distances (Å) <sup>a</sup>	SiH <sub>3</sub> -O-SiH <sub>3</sub> <sup>b</sup>	SiH <sub>3</sub> -S-SiH <sub>3</sub>	SiH <sub>3</sub> -Se-SiH <sub>3</sub>
Si(1)-Y(2)	1.632(5)	2.142(3)	2.253(11)
Si(3)-Y(2)	1.630(5)	2.141(2)	2.291(11)
Si(1)-H(11)		1.30(7)	1.36*
Si(1)-H(12)		1.22(11)	1.47*
Si(1)-H(13)		1.36(14)	1.25*
Si(3)-H(31)		1.29(8)	1.24*
Si(3)-H(32)		1.12(12)	1.36*
Si(3)-H(33)		1.42(9)	1.47*
Si(1) ··· Si(3)	3.086(2)	3.242(3)	3.368(17)
(b) Interbond angles (°) <sup>a</sup>			
Si(1)-Y(2)-Si(3)	142.2(3)	98.4(1)	95.7(4)
Y(2)-Si(1)-H(11)		106(4)	114*
Y(2)-Si(1)-H(12)		113(4)	102*
Y(2)-Si(1)-H(13)		104(7)	83*
Y(2)-Si(3)-H(31)		117(3)	95*
Y(2)-Si(3)-H(32)		107(5)	109*
Y(2)-Si(3)-H(33)		98(4)	109*
(c) Torsion angles (°)			
H(13)-Si(1)-Y(2)-Si(3)	148(4)	-168(7)	-158
H(33)-Si(3)-Y(2)-Si(1)	-153(5)	178(4)	-146

<sup>a</sup> An asterisk denotes hydrogen atom located from difference map and co-ordinates not refined. <sup>b</sup> Ref. 3.

TABLE 4

Intermolecular geometries <sup>a</sup>

(a) Intermolecular contacts at less than the (sum of van der Waals radii + 0.2 Å), where the van der Waals radii are Si 2.10, Se 1.90, S 1.80, and H 1.20 Å

SiH <sub>3</sub> -S-SiH <sub>3</sub>	SiH <sub>3</sub> -Se-SiH <sub>3</sub>
H(13) ··· H(13 <sup>I</sup> )	H(31) ··· H(33 <sup>VII</sup> )
2.43(21)	2.34
S(2) ··· H(13 <sup>I</sup> )	H(13) ··· H(32 <sup>VIII</sup> )
3.10(14)	2.56
Si(3) ··· H(31 <sup>II</sup> )	Se(2) ··· H(11 <sup>IX</sup> )
3.15(8)	3.06
S(2) ··· H(31 <sup>II</sup> )	Se(2) ··· H(11 <sup>X</sup> )
3.16(7)	3.20
Si(1) ··· H(13 <sup>I</sup> )	Si(3) ··· H(12 <sup>XI</sup> )
3.32(15)	3.29
Si(1) ··· S(2 <sup>III</sup> )	Si(1) ··· H(32 <sup>VIII</sup> )
3.548(3)	3.35
S(2) ··· Si(3 <sup>II</sup> )	Si(1) ··· H(13 <sup>XII</sup> )
3.556(2)	3.47
Si(3) ··· Si(3 <sup>IV</sup> )	Se(2) ··· Si(3 <sup>XIII</sup> )
4.182(3)	3.583(11)
Si(3) ··· Si(3 <sup>V</sup> )	Si(1) ··· Se(2 <sup>XII</sup> )
4.387(4)	3.616(12)
	Si(1) ··· Se(2 <sup>VII</sup> )
	4.185(11)
	Si(3) ··· Si(3 <sup>XIV</sup> )
	4.252(13)
	Si(1) ··· Si(1 <sup>XII</sup> )
	4.344(13)

(b) Important intermolecular distances (Å) and angles (°)

	SiH <sub>3</sub> -O-SiH <sub>3</sub> <sup>b</sup>	SiH <sub>3</sub> -S-SiH <sub>3</sub>	SiH <sub>3</sub> -Se-SiH <sub>3</sub>
Si(1) ··· Y(2)	[4.236(6)]	3.548(3) <sup>III</sup>	3.616(12) <sup>XII</sup>
Si(3) ··· Y(2)	3.115(5)	3.556(2) <sup>IV</sup>	3.583(11) <sup>XIV</sup>
Y(2)-Si(1) ··· Y(2)		173.9(2) <sup>III</sup>	172.7(4) <sup>XII</sup>
Y(2)-Si(3) ··· Y(2)	176.6(4)	176.5(2) <sup>IV</sup>	175.6(5) <sup>XIV</sup>
Si(1)-Y(2) ··· Si(1)		99.5(1) <sup>VI</sup>	92.5(4) <sup>X</sup>
Si(1)-Y(2) ··· Si(3)	108.4(2)	106.9(1) <sup>II</sup>	102.4(3) <sup>XIII</sup>
Si(3)-Y(2) ··· Si(1)		127.7(1) <sup>VI</sup>	127.0(3) <sup>X</sup>
Si(3)-Y(2) ··· Si(3)	109.4(2)	91.0(1) <sup>II</sup>	90.0(3) <sup>XIII</sup>
Si(1) ··· Y(2) ··· Si(3)		v <sup>I</sup> 28.9(1) <sup>II</sup>	x <sup>I</sup> 138.7(2) <sup>XIII</sup>

<sup>a</sup> Roman numerals as superscripts refer to the following equivalent positions relative to the reference molecules at *x, y, z*: I 1 - *x*, -*y*, -*z*; II  $\frac{1}{2} + x$ ,  $\frac{1}{2} - y$ , -*z*; III *x*, -*y*,  $\frac{1}{2} + z$ ; IV  $x - \frac{1}{2}$ ,  $\frac{1}{2} - y$ , -*z*; V -*x*, *y*,  $-\frac{1}{2} - z$ ; VI *x*, -*y*,  $z - \frac{1}{2}$ ; VII  $\frac{1}{2} + y$ ,  $\frac{1}{2} - x$ ,  $\frac{1}{4} + z$ ; VIII  $y - \frac{1}{2}$ ,  $\frac{1}{2} - x$ ,  $\frac{1}{4} + z$ ; IX  $\frac{1}{2} - y$ ,  $x - \frac{1}{2}$ ,  $z - \frac{1}{4}$ ; X  $\frac{1}{2} - x$ , *y* -  $\frac{1}{2}$ ,  $\frac{3}{4} - z$ ; XI 1 - *y*, -*x*,  $\frac{1}{2} - z$ ; XII  $\frac{1}{2} - x$ ,  $\frac{1}{2} + y$ ,  $\frac{3}{4} - z$ ; XIII  $x - \frac{1}{2}$ ,  $\frac{1}{2} - y$ ,  $\frac{1}{4} - z$ ; XIV  $\frac{1}{2} + x$ ,  $\frac{1}{2} - y$ ,  $\frac{1}{2} - z$ . <sup>b</sup> Ref. 3.

not include contributions from errors in the cell parameters, but the e.s.d.s in the abstract and in Table 5 do include such contributions. The reliability of the atomic vibration parameters is adversely affected by the lack of direct experimental data for the inter-layer scale factors.

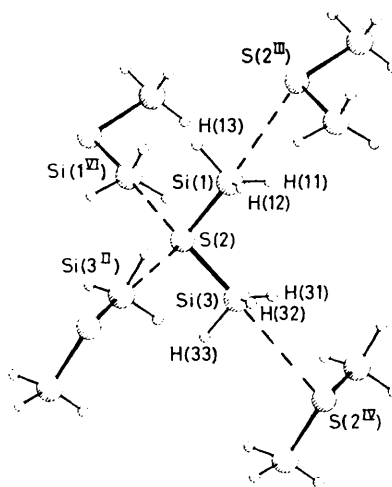


FIGURE 2 View of reference molecule of  $\text{SiH}_3\text{-S-SiH}_3$  showing intermolecular  $\text{Si} \cdots \text{S}$  and  $\text{S} \cdots \text{Si}$  contacts. Roman numeral superscripts are defined in Table 4

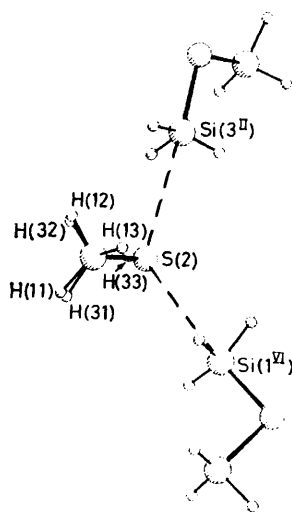


FIGURE 3 Reference molecule of  $\text{SiH}_3\text{-S-SiH}_3$  viewed along the  $\text{Si} \cdots \text{Si}$  vector and showing the  $\text{S} \cdots \text{Si}$  interactions. Roman numeral superscripts are defined in Table 4

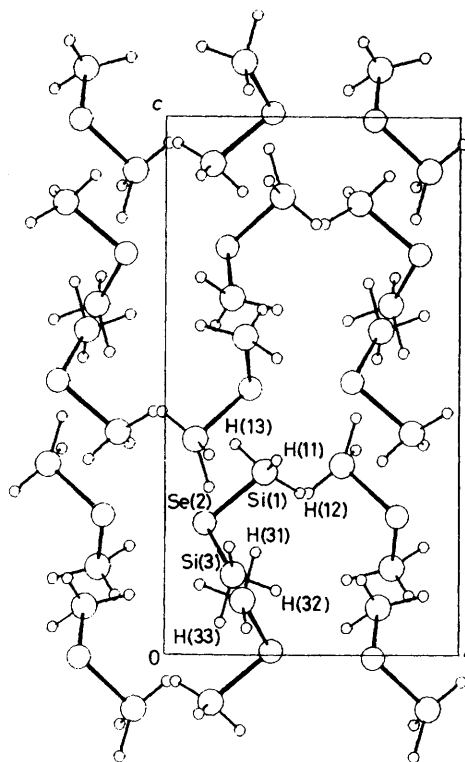


FIGURE 4 Arrangement of molecules in unit cell of  $\text{SiH}_3\text{-Se-SiH}_3$  viewed along  $a$

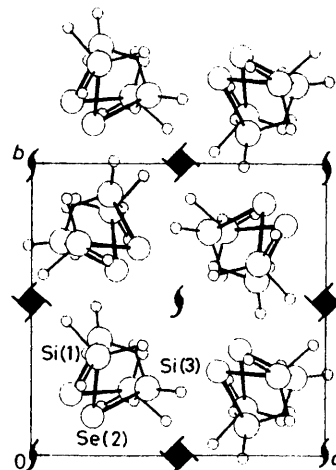


FIGURE 5 Unit cell of  $\text{SiH}_3\text{-Se-SiH}_3$  viewed along  $c$  to show the  $4_3$  axes

TABLE 5

Comparison of $\text{SiH}_3\text{-Y-SiH}_3$ geometries in gas and crystal <sup>a</sup>							
Compound	Phase	Method	$\langle \text{Si-Y} \rangle$ (Å)	Si-Y-Si (°)	Si(1) $\cdots$ O(2') <sup>b</sup> (Å)	Si(3) $\cdots$ O(2'') <sup>b</sup> (Å)	Ref.
$\text{SiH}_3\text{-O-SiH}_3$	Gas	e.d.	1.634(2)	144.1(9)			2
$\text{SiH}_3\text{-O-SiH}_3$	Crystal	X-ray	1.631(6)	142.2(3)	[4.24(1)] <sup>c</sup>	3.12(1)	3
$\text{SiH}_3\text{-S-SiH}_3$	Gas	e.d.	2.136(2)	97.4(7)			4
$\text{SiH}_3\text{-S-SiH}_3$	Crystal	X-ray	2.142(7)	98.4(3)	3.55(1)	3.56(1)	This work
$\text{SiH}_3\text{-Se-SiH}_3$	Gas	e.d.	2.275(4)	96.6(7)			5
$\text{SiH}_3\text{-Se-SiH}_3$	Crystal	X-ray	2.27(2)	95.7(5)	3.62(2)	3.58(2)	This work

<sup>a</sup> E.s.d.s given here include contributions from errors in the cell parameters (but those in Tables 1—4 do not). <sup>b</sup> Intermolecular contacts. <sup>c</sup> Not stereospecific.

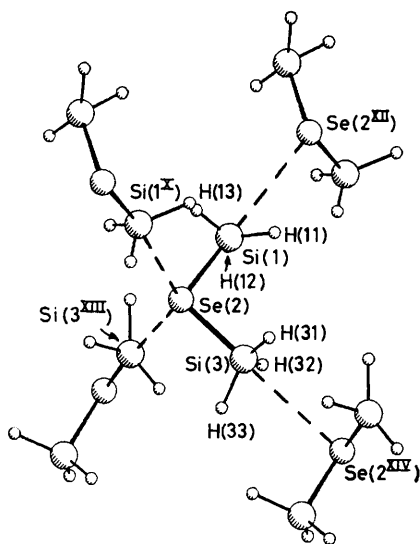


FIGURE 6 View of reference molecule of  $\text{SiH}_3\text{-Se-SiH}_3$  showing intermolecular  $\text{Si}\cdots\text{Se}$  and  $\text{Se}\cdots\text{Si}$  contacts. Roman numeral superscripts are defined in Table 4

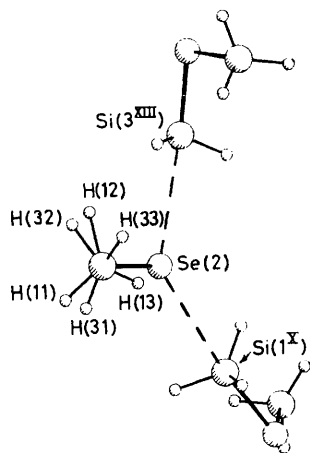


FIGURE 7 Reference molecule of  $\text{SiH}_3\text{-Se-SiH}_3$  viewed along the  $\text{Si}\cdots\text{Si}$  vector and showing the  $\text{Se}\cdots\text{Si}$  interactions. Roman numeral superscripts are defined in Table 4

#### DISCUSSION

Table 5 compares bond lengths and angles determined for  $\text{SiH}_3\text{-Y-SiH}_3$  species ( $\text{Y} = \text{O}, \text{S}, \text{or Se}$ ) in gaseous and crystalline phases. Differences between molecular geometries in the gas and solid are slight. The lengths of the  $\text{Si}(1)\text{-Se}(2)$  and  $\text{Se}(2)\text{-Si}(3)$  bonds in crystalline  $\text{SiH}_3\text{-Se-SiH}_3$  cannot be said to be different if one uses a significance limit of  $3\sigma$ ;  $\Delta(l_1 - l_2) = 0.038 \text{ \AA}$  with e.s.d. of  $0.016 \text{ \AA}$ . The average length of the  $\text{Si-Se}$  bonds in the solid is  $2.27(2) \text{ \AA}$ . The hydrogen atoms adopt slightly different conformations in each of the three crystal structures (see Figures 3, 7, and 9); the arrangement in the sulphide structure is the most symmetrical, very close to  $C_{2v}$  molecular symmetry.

The striking feature of all three crystal structures is the presence of long, but directionally specific, intermolecular

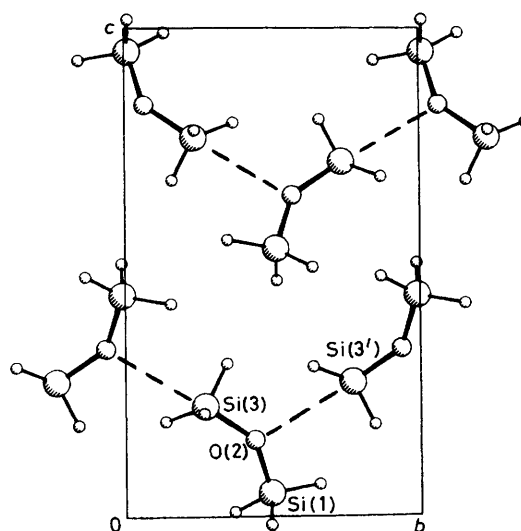


FIGURE 8 Unit cell of  $\text{SiH}_3\text{-O-SiH}_3$  viewed down  $a$  showing the intermolecular  $\text{Si}\cdots\text{O}$  and  $\text{O}\cdots\text{Si}$  contacts

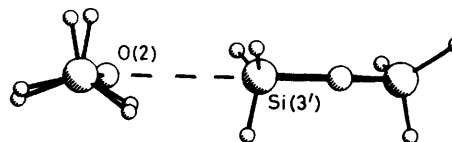


FIGURE 9 Molecule of  $\text{SiH}_3\text{-O-SiH}_3$  viewed along the  $\text{Si}\cdots\text{Si}$  vector to show the  $\text{O}\cdots\text{Si}$  interaction

$\text{Si}\cdots\text{Y}$  contacts. The sulphide and selenide have similar intermolecular geometries. Each Si atom forms one  $\text{Si}\cdots\text{Y}$  interaction; the  $\text{Si}\cdots\text{Y}$  distances are  $0.35\text{--}0.4 \text{ \AA}$  less than the sum of van der Waals radii and the angles  $\text{Y-Si}\cdots\text{Y}$  are very close to  $180^\circ$ . Each Y atom has two  $\text{Y}\cdots\text{Si}$  interactions. Although the angles subtended at Y by the two close and two distant Si atoms are irregular, the angles are tending towards tetrahedral values.

The intermolecular contacts in crystalline  $\text{SiH}_3\text{-O-SiH}_3$  are simpler. Here only one Si atom,  $\text{Si}(3)$ , forms an intermolecular interaction to oxygen. This  $\text{Si}\cdots\text{O}$  distance is  $0.5 \text{ \AA}$  less than the sum of van der Waals radii, and the  $\text{O-Si}\cdots\text{O}$  angle is close to  $180^\circ$ . It follows that the oxygen atom also has only one  $\text{O}\cdots\text{Si}$  contact. The co-ordination geometry at oxygen involves two close and one distant Si atoms with all four atoms lying in the same plane and with the  $\text{O}\cdots\text{Si}$  vector almost bisecting the  $\text{Si-O-Si}$  angle.

In summary therefore the sulphide and selenide structures involve Si atoms with  $4 + 1$  co-ordination and S (or Se) atoms with  $2 + 2$  co-ordination. The oxide structure has one Si atom with four-co-ordination, the other Si atom with  $4 + 1$  co-ordination, and the oxygen is  $2 + 1$  co-ordinated. That the co-ordination at oxygen is  $2 + 1$  while the comparable co-ordinations at S and Se are  $2 + 2$  is consistent with the idea that in the oxide (but not in the sulphide or selenide) the effective number of lone pairs of electrons at oxygen is reduced by multiple bonding within the *intra*-molecular  $\text{Si-O}$  bonds.

[1/792 Received, 18th May, 1981]

Although the Si...Y contacts are appreciably less than the sum of van der Waals radii these contacts are nevertheless considerably greater (by 1.3—1.5 Å) than normal bonded distances. The interactions must be very weak, yet they do have well defined directional properties and a dominant influence on crystal packing. During previous consideration of crystal structures involving 4 + 1 co-ordination at Si we adopted the method of structural correlations<sup>13</sup> to analyse the co-ordination geometries in terms of an S<sub>N</sub>2 type of reaction pathway.<sup>14</sup> This pathway would lead from tetrahedral four-co-ordination to trigonal-bipyramidal five-co-ordination. Short interactions seem most likely to occur when the 'donor' atom is nitrogen and when the 'acceptor' atom Si is present as an SiH<sub>3</sub> group. For instance the pentameric structure of Me<sub>2</sub>N-SiH<sub>3</sub> probably involves true trigonal-bipyramidal co-ordination at Si: all the Si-N and Si...N distances are ca. 1.98 Å.<sup>15</sup> On this basis oxygen seems a less effective donor; the shortest O...SiH<sub>3</sub> contact we have determined is 2.72 Å.<sup>16</sup> There are now plenty of examples of Si...N and Si...O interactions. However, both oxygen and nitrogen are first-row 'hard-atom' donors; much of the significance of the Si...S and Si...Se interactions reported here is that the donor atoms are from the second and third rows.

We thank the S.R.C. for financial support and Mr. S. G. D. Henderson for samples of disilyl sulphide and disilyl selenide.

## REFERENCES

- <sup>1</sup> J. R. Durig, M. J. Flanagan, and V. F. Kalasinsky, *J. Chem. Phys.*, 1977, **66**, 2775.
- <sup>2</sup> A. Almenningen, O. Bastiansen, V. Ewing, K. Hedberg, and M. Traetteberg, *Acta Chem. Scand.*, 1963, **17**, 2455.
- <sup>3</sup> M. J. Barrow, E. A. V. Ebsworth, and M. M. Harding, *Acta Crystallogr., Sect. B*, 1979, **35**, 2093.
- <sup>4</sup> A. Almenningen, K. Hedberg, and R. Seip, *Acta Chem. Scand.*, 1963, **17**, 2264.
- <sup>5</sup> A. Almenningen, L. Fernholt, and H. M. Seip, *Acta Chem. Scand.*, 1968, **22**, 51.
- <sup>6</sup> SHELX, Program for Crystal Structure Determination, G. M. Sheldrick, University Chemical Laboratory, Cambridge, 1976.
- <sup>7</sup> 'International Tables for X-Ray Crystallography,' Kynoch Press, Birmingham, 1974, vol. 4, p. 99.
- <sup>8</sup> D. T. Cromer and J. B. Mann, *Acta Crystallogr., Sect. A*, 1968, **24**, 321.
- <sup>9</sup> R. F. Stewart, E. R. Davidson, and W. T. Simpson, *J. Chem. Phys.*, 1965, **42**, 3175.
- <sup>10</sup> D. T. Cromer and D. J. Liberman, *J. Chem. Phys.*, 1970, **53**, 1891.
- <sup>11</sup> J. M. Stewart, 'X-RAY '76,' Technical Report TR-446, University of Maryland, 1976.
- <sup>12</sup> PLUTO, Program for Plotting Crystal and Molecular Structures, W. D. S. Motherwell, University Chemical Laboratory, Cambridge.
- <sup>13</sup> H.-B. Bürgi, *Angew. Chem. Int. Ed.*, 1975, **14**, 460.
- <sup>14</sup> M. J. Barrow, E. A. V. Ebsworth, and M. M. Harding, *J. Chem. Soc., Dalton Trans.*, 1980, 1838.
- <sup>15</sup> R. Rudman, W. C. Hamilton, S. Novick, and T. D. Goldfarb, *J. Am. Chem. Soc.*, 1967, **89**, 5157.
- <sup>16</sup> M. J. Barrow, S. Craddock, E. A. V. Ebsworth, and D. W. H. Rankin, *J. Chem. Soc., Dalton Trans.*, 1981, 1988.